European Journal of Cell Biology 102 (2023) 151343

Contents lists available at ScienceDirect

European Journal of Cell Biology

journal homepage: www.elsevier.com/locate/ejcb

3D environment controls H3K4 methylation and the mechanical response of the nucleus in acute lymphoblastic leukemia cells

Raquel González-Novo [a], Ana de Lope-Planelles [a], María Pilar Cruz Rodríguez [a], África González-Murillo [b,c], Elena Madrazo [a], David Acitores [d], Mario García de Lacoba [e], Manuel Ramírez [b,c], Javier Redondo-Muñoz [a,*]

[a] Department of Molecular Medicine, Centro de Investigaciones Biológicas Margarita Salas (CIB Margarita Salas-CSIC), Madrid, Spain
[b] Oncolohematology Unit, Hospital Universitario Niño Jesús, Madrid, Spain
[c] Health Research Institute La Princesa, Madrid, Spain
[d] Institute of Animal Breeding and Genetics, University of Veterinary Medicine, Vienna, Austria
[e] Bioinformatics and Biostatistics Unit, Centro de Investigaciones Biológicas Margarita Salas (CIB Margarita Salas-CSIC), Madrid, Spain

ARTICLE INFO

Keywords:
Cell migration
Epigenetics
Nuclear deformability
Acute lymphoblastic leukemia
Cell invasion

ABSTRACT

Acute lymphoblastic leukemia (ALL) is the most common pediatric cancer, and the infiltration of leukemic cells is critical for disease progression and relapse. Nuclear deformability plays a critical role in cancer cell invasion through confined spaces; however, the direct impact of epigenetic changes on the nuclear deformability of leukemic cells remains unclear. Here, we characterized how 3D collagen matrix conditions induced H3K4 methylation in ALL cell lines and clinical samples. We used specific shRNA and chemical inhibitors to target WDR5 (a core subunit involved in H3K4 methylation) and determined that targeting WDR5 reduced the H3K4 methylation induced by the 3D environment and the invasiveness of ALL cells *in vitro* and *in vivo*. Intriguingly, targeting WDR5 did not reduce the adhesion or the chemotactic response of leukemia cells, suggesting a different mechanism by which H3K4 methylation might govern ALL cell invasiveness. Finally, we conducted biochemical, and biophysical experiments to determine that 3D environments promoted the alteration of the chromatin, the morphology, and the mechanical behavior of the nucleus in ALL cells. Collectively, our data suggest that 3D environments control an upregulation of H3K4 methylation in ALL cells, and targeting WDR5 might serve as a promising therapeutic target against ALL invasiveness in vivo.

1. Introduction

Acute lymphoblastic leukemia (ALL) is the most common pediatric cancer; despite current therapies have improved the outcomes for children with ALL up to 90%, a proportion of patients still experience therapy failure and fatal relapse (Inaba et al., 2013). Leukemic cells interact with their surrounding environment, which provides biochemical and physical signals that control leukemia initiation, proliferation, survival, and tissue infiltration (Vadillo et al., 2018). Migration through these 3D environments promotes nuclear alterations such as gene regulation, epigenetic changes, and DNA damage markers (Shivashankar, 2011; Yamada and Sixt, 2019). This is particularly important for the nucleus, which acts as a cellular mechanosensor to allow cancer cells to deform and squeeze through physical barriers, such as the interstitial space and endothelial barriers during their infiltration into other organs (Kirby and Lammerding, 2018; Wolf et al., 2013).

Epigenetics are modifications such as histone alterations, DNA methylation, and ncRNA that alter the chromatin structure without modifying the DNA sequence (Kouzarides, 2007). The potential importance of epigenetic machinery in human pathologies is widely recognized (Portela and Esteller, 2010). Despite the fundamental role of epigenetics in controlling the transcriptional stage and DNA homeostasis, non-genomic functions of epigenetic changes have been proposed, including the direct impact of epigenetic changes on the physical properties of the nucleus (Bustin and Misteli, 2016). Although, genetic and epigenetic studies have identified potential prognosis markers and therapeutic targets against leukemia initiation and progression (Figueroa et al., 2013; Almamun et al., 2015); the interplay between the surrounding environment and epigenetic changes induced in ALL cells remains functionally unexplored. The methylation of the histone H3 in

* Corresponding author.
E-mail address: javier.redondo@cib.csic.es (J. Redondo-Muñoz).

https://doi.org/10.1016/j.ejcb.2023.151343
Received 14 March 2023; Received in revised form 30 June 2023; Accepted 19 July 2023
Available online 23 July 2023

the residue K4 (H3K4) is a critical epigenetic marker for transcriptional-dependent and -independent functions and contributes to genome stability and cancer progression (Hu et al., 2017; Chong et al., 2020; Clouaire et al., 2012). WDR5 (WD40-repeat protein 5) is a nuclear protein involved in multiple cellular functions (Trievel and Shilatifard, 2009); although the most prominent is its binding to MLL/SET histone methyltransferase complexes to H3K4 methylation (Dou et al., 2006). Furthermore, WDR5 is involved in the malignant transformation and progression of multiple cancers, including leukemia (Ge et al., 2016). In addition, WDR5 regulates H3K4 methylation and cancer metastasis, and cell motility in different environments, including 3D conditions (Tan et al., 2017; Wang et al., 2018).

Here, we characterized those 3D environmental conditions promoted upregulation of H3K4 methylation in ALL cells. We demonstrated that targeting WDR5 reduced leukemia cell infiltration and migration *in vitro* and *in vivo*. Notably, we found a correlation between the expression of WDR5 and other cell receptors involved in ALL migration, such as CXCR4; nonthelesss, we observed that targeting WDR5 did not reduce the chemotactic response of ALL cells, suggesting a specific role of WDR5 for cell migration in 3D conditions. We analyzed fast transcriptional changes in the genomic profile of migrating ALL cells in 3D confined conditions and found that the H3K4 methylation induced by 3D environments was independent of other transcriptional changes. We performed a molecular and biomechanical characterization of the nucleus of ALL cells and found that 3D culture conditions influence the global chromatin structure, the morphology, and the physical deformability of the nucleus, which might be critical for cell migration across confined spaces. Together, our results strengthen the notion that ALL cells respond to their surrounding environment promoting nuclear changes, which might be a promising therapeutic target against leukemia invasiveness.

2. Methods

2.1. Cells and cell culture

The human CCRF-CEM (RRID: CVCL_0207) and Reh (RRID: CVCL_1650) ALL cell lines were from ATCC, American Type Culture Collection. Both cell lines were monthly tested for mycoplasm contamination and yearly subjected to cell identification by single nucleotide polymorphism. ALL primary cells were obtained from patients under 16 years old with informed consent for research purposes at Hospital Universitario Niño Jesús (Table S1). This study was reviewed and approved by the ethics committee of the CSIC and Hospital Niño Jesús, and written informed consent was obtained from all parents, according to the Helsinki Declaration of 1975. ALL diagnosis and treatment were defined according to SEHOP-PETHEMA 2013 (Spanish Program for the Treatment of Hematologic Diseases). All cells were cultured in RPMI 1640 medium with L-glutamine and 25 mM Hepes (Sigma Aldrich, St. Louis, MO, USA) and 10 % fetal bovine serum (Sigma-Aldrich) and maintained in 5 % CO_2 and 37 ºC.

Cells were cultured in suspension, on plates coated with VCAM-1 or embedded in a collagen matrix. For 3D matrix, collagen type I from bovine were reconstituted at 1.7 mg/ml in RPMI and neutralized with 7.5 % NaHCO3 and 25 mM Hepes. Cells were added to the collagen solution before polymerization at 37 °C for 1 h. In some cases, cells were preincubated with specific chemical inhibitors and the medium was also supplemented with these inhibitors.

2.2. Cell penetration assay

A 100 μl collagen matrix was reconstituted at 1.7 mg/ml in RPMI, neutralized with 7.5% NaHCO3 and 25 mM Hepes and allowed to polymerize inside transwell inserts (5 μm, Costar). 3×10^5 cells were pretreated or not with OICR-9429 for 1 h in serum-free RPMI, or transfected with control- and WDR5-shRNAs for 24 h before seeding onto a collagen gel. RPMI medium with 10% of FBS was added to the bottom chamber of the transwell as chemoattractant. After 24 h, invading cells were fixed with 4 % PFA for 1 h, permeabilized with 0.5 % Triton-X-100 in PBS for 30 min and stained with propidium iodide. Invading cells were imaged with a sCMOS Orca-Flash 4.0LT camera (Hamamatsu) coupled 5 to an inverted DMi8 microscope (Leica), capturing serial z- stacks every 10 μm with a 10 × objective (dry ACS APO 10x/NA 0.3). Percentage of penetrating cells in each range of distances was quantified with FIJI software (National Institute Health, US).

2.3. In-vivo short-term leukemia homing assay

NOD-SCID-Il2rg-/- (NSG) mice (*Mus musculus*), were purchased at Charles River (France), and bred and maintained at the Servicio del Animalario del Centro de Investigaciones Energéticas, Medioambientales y Tecnológicas (CIEMAT) with number 28079–21A. All procedures for animal experiments were approved by the Committee on the Use and Care of Animals and carried out in strict accordance with the institution guidelines and the European and Spanish legislations for laboratory animal care. 5×10^6 control and WDR5 inhibited CCRF-CEM cells were labeled with Cell Tracker Far Red (1 μM) and CFSE (5 μM), respectively. After 30 min, cells were mixed and intravenously (IV) administered to 15 weeks-old non-conditioned NSG mice. Sacrifice was performed 3 h after injection. Bone marrow from femurs and spleens were extracted, processed through mechanical disaggregation and stained cells were resuspended in the PBS. Samples were acquired in a FacsCanto II (BD, San Jose, CA) cytometer and the number of labeled cells analyzed using FacsDiva software. Transfected control (labeled with Cell Tracker Far Red) and WDR5 shRNA (labeled with CFSE) CCRF-CEM cells were mixed and intravenously administered to NSG mice. Organs were extracted, processed through mechanical disaggregation and stained cells were resuspended in the PBS and analyzed by flow cytometry. Also, the distribution among the tissues of colonizing cells was studied by sample fixation in formaldehyde, frozen in OCT (optimum cutting temperature) and serial cryostat sections were stained with Dapi and directly imaged with a 20 × objective.

3. Results

3.1. The 3D environment promotes H3K4 methylation in ALL cells, which control their invasiveness in vitro through WDR5

We first determined whether 3D conditions might alter chromatin changes in ALL cells. We cultured two ALL cell lines (CCRF-CEM and Reh) in suspension or embedded them in a 3D collagen matrix and found that the 3D environment upregulated the levels of H3K4me3 in both cell lines compared to cells cultured in suspension (Fig. 1A, B). Furthermore, we also confirmed that 3D culture conditions upregulated the levels of H3K4me3 in primary T- and B-ALL cells within 1 h. (Fig. S1A). We confirmed that 3D culture conditions did not alter the levels of other histone markers and c-myc in ALL cells at the times studied (Fig. S1B). Then, we cultured ALL cells in 3D conditions for different times and confirm that cells embedded in a collagen matrix were able to upregulate H3K4 methylation within 1 h (Fig. S1C). To explore whether 3D conditions promoted permanent or transient changes in the levels of H3K4me3, we cultured ALL cells in 3D conditions, collected them, and cultured them in suspension for an additional hour. Interestingly, the H3K4 methylation induced by 3D conditions was reversible in the absence of confined environments (Fig. S1D). Together, this set of evidence suggests that 3D conditions might promote a transient upregulation of H3K4me3 levels in ALL cells.

It has been reported that targeting WDR5 could block the migration of cancer cells (Punzi et al., 2019). By using a specific inhibitor against H3K4 methylation and the WDR5-MLL interaction, called OICR-9429 (Grebien et al., 2015), we confirmed that the H3K4me3-induced by 3D conditions in ALL cells was dependent on WDR5 (Fig. 1C). Then, to

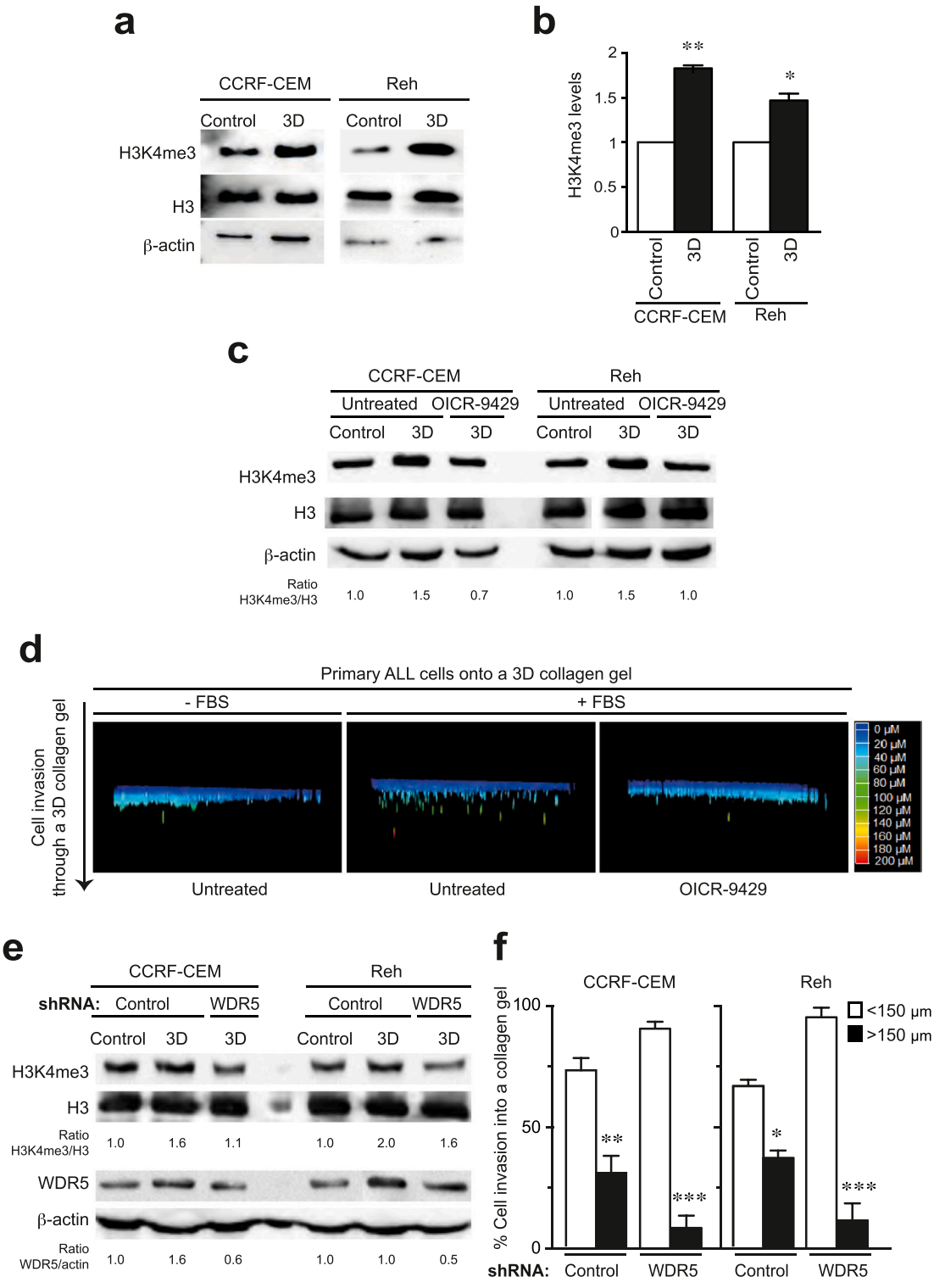

Fig. 1. 3D conditions control the H3K4 methylation and infiltration of ALL cells. (A) CCRF-CEM and Reh cells were cultured in suspension (Control) or embedded in a 3D collagen matrix (3D). After 1 h, the protein levels of H3K4me3 were tested by western blotting. (B) Graph shows the H3K4 methylation levels normalized to loading controls. Mean n = 3 ± SEM. (C) CCRF-CEM and Reh cells were pretreated or not with 1 μM OICR-9429 (WDR5 inhibitor) and cultured in suspension or in 3D conditions. Then, H3K4me3 levels were tested by western blotting. Numbers represent the H3K4me3/H3 ratio after normalizing control cell values to 1. (D) ALL primary cells were pretreated or not with 1 μM OICR-9429, seeded on the top of the collagen matrix, and allowed to invade into the collagen in response to serum (FBS, fetal bovine serum) for 24 h. Cells were fixed and stained with Propidium Iodide. Images show rendering reconstruction from serial confocal sections of the cell invasion into the collagen. (E) CCRF-CEM and Reh cells were transfected with control or WDR5 shRNAs for 24 h and cultured in suspension or in 3D conditions. Protein levels were determined by western blotting. Numbers represent the H3K4me3/H3 and WDR5/β-actin ratio after normalizing control cell values to 1. (F) Control or WDR5-depleted CCRF-CEM and Reh cells were seeded on the top of collagen matrix and allowed to penetrate into the collagen in response to FBS. Graphs show the cell invasion into the collagen. (*) $P < 0.05$, (**) $P < 0.005$, (***) $P < 0.001$.

determine the functional consequences of H3K4 methylation on leukemia invasiveness, we seeded control or OICR-9429-treated ALL cells onto the surface of 3D collagen matrices and their invasion was visualized by confocal sections. We carried out 3D rendering reconstructions and color-coded the depth of invasion of ALL cells and found that OICR-9429 treatment reduced the invasive deepness of primary ALL samples (Fig. 1D and Fig. S2A) and both ALL cell lines (Fig. S2B and S2C). To further validate our observations, we depleted WDR5 expression in both cell lines (Fig. S2D) and confirmed that WDR5 depletion impaired the H3K4 methylation induced by 3D conditions (Fig. 1E) and reduced the invasiveness of ALL cells into the collagen matrix (Fig. 1F). Together, our data indicate that ALL cells increased their levels of H3K4 methylation in 3D conditions, and targeting WDR5 might serve to reduce the infiltration of ALL cells into dense extracellular environments.

3.2. *WDR5 inhibition impairs the infiltration of ALL cells in vivo*

To enhance the physiological relevance of targeting WDR5 during ALL migration, we mixed control and WDR5-depleted cells and injected them into the tail vein of recipient immunodeficient NSG (NOD scid gamma) mice. We quantified the percentage of ALL cells in the spleen and the bone marrow at 3 h post-injection (Fig. 2A) and confirmed that WDR5 silencing reduced the homing of ALL cells into these organs (Fig. 2B). Likely, OICR-9429 pretreatment also inhibited the homing of ALL cells into the spleen (Fig. S3A and S3B). We next assessed whether targeting WDR5 might have an effect on the specific infiltration and localization of ALL cells into the different tissues. Our analyses demonstrated that OICR-9429 treatment reduced the total number of ALL cells reaching the tissues without affecting their distribution throughout the tissues (Fig. 2C). To discard that OICR-9429 treatment might be affecting the cell migration *via* cell cycle regulation or apoptosis, we incubated ALL cell lines with OICR-9429 and confirmed that their cell cycle progression and survival were not affected at 3 h (data not shown) and 24 h (Fig. 2D and E). Our results might suggest that OICR-9429 treatment might induce a small increment in the levels of cyclin D1 (a G1 phase marker) without further affecting the levels of phospho-H2AX (a DNA damage marker) (Fig. 2F and Fig. S3C). To further validate these results, we confirmed that WDR5 depletion did not alter the levels of these proteins, nor the cell cycle progression (Fig. S3D and S3E). Taken together, these data propose that targeting WDR5 might have an impact on the infiltration and dissemination of ALL cells *in vivo* without affecting their viability.

3.3. *WDR5 expression is associated with cell migration molecules in samples of ALL patients*

Next, we interrogated whether the effect of targeting WDR5 on leukemia invasiveness might be due to altered chemotaxis of ALL cells, as leukemia cell migration depends on integrins and the chemotactic response of leukemia cells (Vadillo et al., 2018). Some chemokine receptors are critical modulators of leukemia invasion and might serve as prognostic markers of ALL, including CXCR4 (C-X-C Motif Chemokine Receptor 4) and CCR7 (C-C Motif Chemokine Receptor 7) (Crazzolara et al., 2001; Corcione et al., 2006; Buonamici et al., 2009). First, we analyzed the expression of WDR5 in mRNA samples from a cohort of 15 B-ALL patients, and found a positive correlation between the mRNA levels of WDR5 and CXCR4 in samples from patients with ALL (Fig. 3A); however, we did not observe a similar correlation with CCR7 (Fig. S4A). As mRNA expression might not correlate with the surface expression and function of cell receptors, we tested the expression levels of CXCR4 at the surface of ALL cells treated with OICR-9429 or depleted for WDR5 and found no significant differences upon WDR5 targeting (Fig. 3B and S4B). The sphingosine-1-phosphate (S1P) modulates migration of lymphocytes and tumor cells (Spiegel and Kolesnick, 2002; García-Bernal et al., 2013; Golan et al., 2013), and we confirmed that both ALL cell lines expressed low levels of S1PR1 (sphingosine-1-phosphate receptor 1, also designed as EDG-1, endothelial differentiation gene-1) and OICR-9429 treatment did not alter its levels (Fig. S4C). Furthermore, we confirmed that the levels of CXCR4 and S1PR1 remained unaltered in total lysates of CCRF-CEM and Reh cells upon WDR5 silencing or inhibition (Fig. S4D). As expected from the qPCR analysis, we also observed no significant differences in the levels of CCR7 at the surface of ALL cells treated with OICR-9429 (Fig. S4E). Then, we assessed the chemotactic response of ALL cells by treating primary samples and ALL cell lines with OICR-9429. We observed that WDR5 inhibition did not reduce the migration, and even increased the migration of ALL towards FBS (Fig. 3C). We also confirmed that WDR5 depletion did not reduce the migration of CCRF-CEM and Reh cells (Fig. S4F). As WDR5 targeting seemed to increase slightly the migration of ALL cells to chemoattracts, we specifically analyzed the chemotactic response of ALL cells to CXCL12 (the ligand for CXCR4), and found that targeting WDR5 might promote a slight increment in the migratory response of ALL cells to CXCL12 (Fig. 3D).

The integrin VLA-4 (very late antigen 4) has been proposed as a prognosis marker for ALL (Crazzolara et al., 2001; Shalapour et al., 2011). Having observed a potential link between CXCR4 and WDR5 expression, we next compared WDR5 expression and the mRNA levels of the integrin α4 (a subunit of the integrin VLA4). Although we did not observe a correlation between both proteins (Fig. S5A), we found that those patients stratified as high-risk (poor early cytological response, or minimal residual disease level $\geq$ 0.05 % at the end of reinduction) might suggest a positive correlation between the mRNA levels of WDR5 and α4 subunit (Fig. S5B). Then, we characterized whether targeting WDR5 might impair ALL cell migration *via* VLA4. To address this; we determined that targeting WDR5 did not affect the surface expression of α-subunit of the integrin (Fig. 3E and S5C). As expected, when we determined the activation stage of the β1-subunit of the integrin VLA4, we found only slight differences in ALL cells treated with OICR-9429 or depleted for WDR5 (Fig. S5D and S5E). To determine whether the effect of targeting WDR5 on ALL cell invasiveness was independent of VLA4, we analyzed the cell migration induced by VCAM-1 (Vascular cell adhesion protein 1, a specific ligand of VLA4), and found that OICR-9429 treatment did not reduce the migration of ALL cells induced by (Fig. 3F).

These results indicate that WDR5 expression may correlate with migratory molecules in ALL cells; although its activity was not required for ALL cell migration mediated by these receptors. This supports the notion that targeting WDR5 might impede the dissemination of ALL cells by a different mechanism.

3.4. *H3K4 methylation induced by 3D conditions is dependent on myosin activation and controls cell motility through confined conditions*

The cell cytoskeleton acts as a mechanotransducer to integrate external stimuli from the surrounding microenvironment into the nucleus of cancer cells (Dahl et al., 2008). As actin polymerization is known to control adhesive structures related to cancer cell migration and adhesion (Kelley et al., 2019), we interrogated about the potential molecular links between WDR5 and the cytoskeleton of ALL cells. We found that targeting WDR5 induced only minimal changes in the level of F-actin of CCRF-CEM and Reh cells (Fig. 4A and S6A). Furthermore, we also confirmed that OICR-9429 treatment did not affect the levels of F-actin in primary ALL cells (Fig. S6B). MLCK (myosin light chain kinase) activity and myosin phosphorylation are critical for the H3K4 methylation induced by WDR5 (Wang et al., 2018; Downing et al., 2013). We observed that 3D conditions increased the levels of phospho-myosin in ALL cells, and the specific inhibitor for MLCK (ml-7) impaired this increment (Fig. S6C). Furthermore, we confirmed that the treatment with ml-7 also impaired the upregulation of H3K4me3 induced by 3D conditions in ALL cells (Fig. 4B, C). To better define the relationship between WDR5 and the myosin activity, we explored how

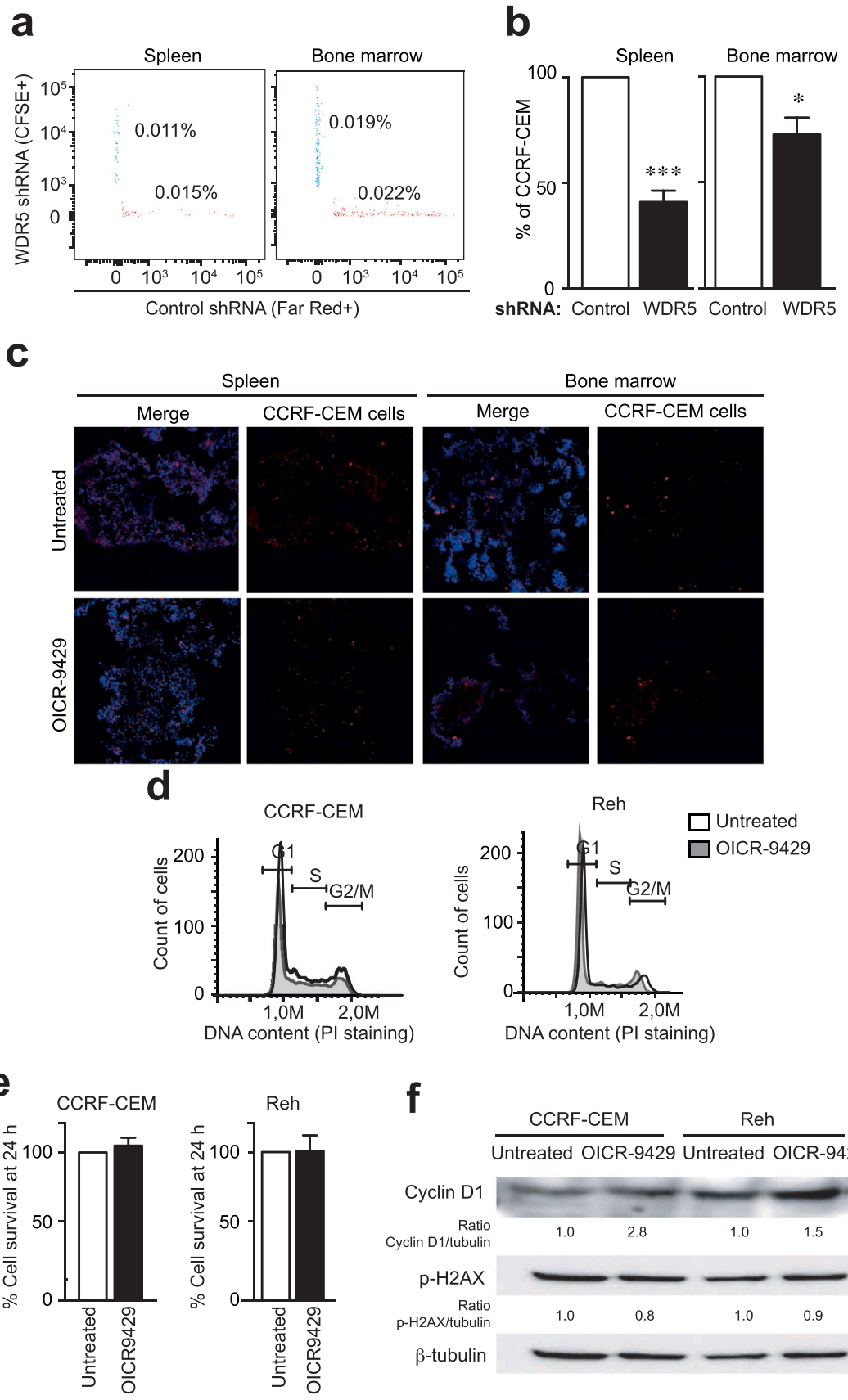

(caption on next page)

Fig. 2. Targeting WDR5 impairs the capacity of ALL to reach the spleen and the bone marrow *in vivo*. (A) CCRF-CEM cells transfected with control (CFSE+) or WDR5 (Cell Tracker Far Red+) shRNAs were mixed 1:1 and injected into the tail vein of immunodeficient recipient mice. After 3 h, animals were sacrificed and the homing of labeled cells into the spleen and the bone marrow was determined by flow cytometry. (B) Graphs show the percentage of labeled leukemia cells according to the total number of events. Mean n = 4 ± SEM. (C) Representative images of tissue sections from the spleen and the bone marrow of recipient mice injected with CCRF-CEM cells pretreated or not with 1 μM OICR-9429. (D) CCRF-CEM and Reh cells were treated with 1 μM OICR-9429 for 24 h. Then, cells were stained with PI and the cell cycle progression was analyzed by flow cytometry. Graphs show the G1, S, and G2/M phases according to DNA content. (E) CCRF-CEM and Reh cells were treated with 1 μM OICR-9429 for 24 h, collected and fixed. Cell viability was determined by Annexin V and PI staining. (F) CCRF-CEM and Reh cells were cultured in the presence of OICR-9429. After 24 h, cell lysates were resolved by western blotting. Numbers represent the Cyclin D1/tubulin and pH2AX/tubulin ratio after normalizing untreated cell values to 1. (*) P < 0.05, (***) P < 0.001.

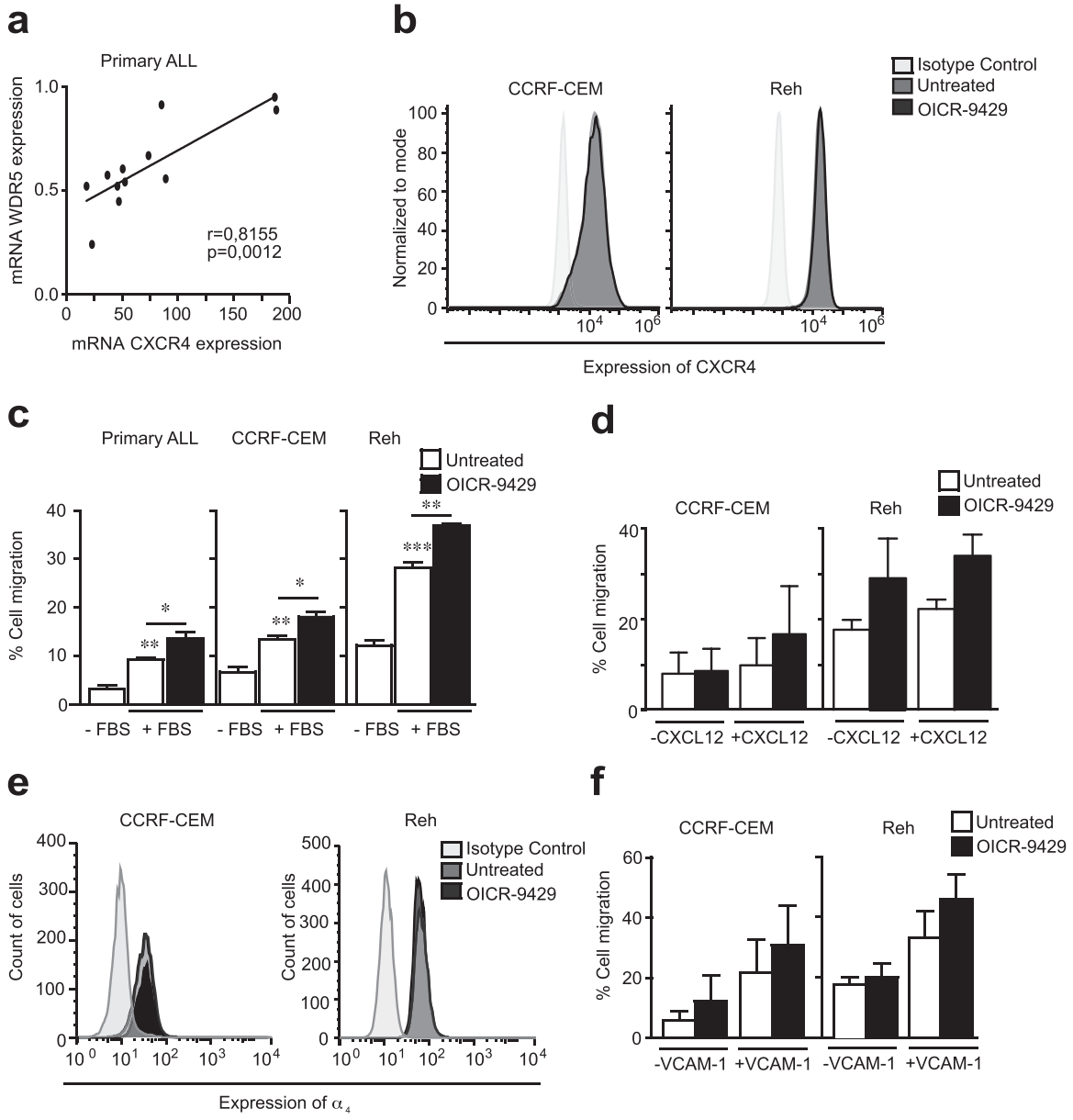

Fig. 3. Targeting WDR5 does not reduce the migration of ALL cells in response to chemokines or integrins. (A) WDR5 and CXCR4 expression (mRNA) in B-ALL cells from patients (n = 12) were analyzed by RT-qPCR. Expression levels were normalized by TBP and the graph shows the correlation between both molecules. Pearson's correlation coefficient (r) and P-value are shown. (B) CCRF-CEM and Reh cells were pretreated or not with 1 μM OICR-9429. Then, the expression levels of CXCR4 were determined by flow cytometry. (C) ALL cells pretreated or not with 1 μM OICR-9429 were seeded on the top of Transwell chambers and allowed to migrate in response to FBS. Cells were collected from the bottom chamber after 24 h and quantified. Mean n = 3 replicates ± SEM. (D) CCRF-CEM and Reh cells pretreated or not with 1 μM OICR-9429 were seeded on the top of Transwell chambers and CXCL12 (150 ng/ml) was added to the bottom Transwell chambers. Cells were collected from the bottom chamber after 24 h and spontaneous migration was quantified. Mean n = 3 replicates ± SEM. (E) Flow cytometry expression of α4 subunit at the surface of CCRF-CEM and Reh cells pretreated with 1 μM OICR-9429. (F) CCRF-CEM and Reh cells pretreated or not with 1 μM OICR-9429 were seeded on the top of Transwell chambers coated with VCAM-1 (10 μg/ml). Cells were collected from the bottom chamber after 24 h and spontaneous migration induced by VCAM-1 adhesion was quantified. Mean n = 4 replicates ± SEM. (*) P < 0.05, (**) P < 0.01, (***) P < 0.001.

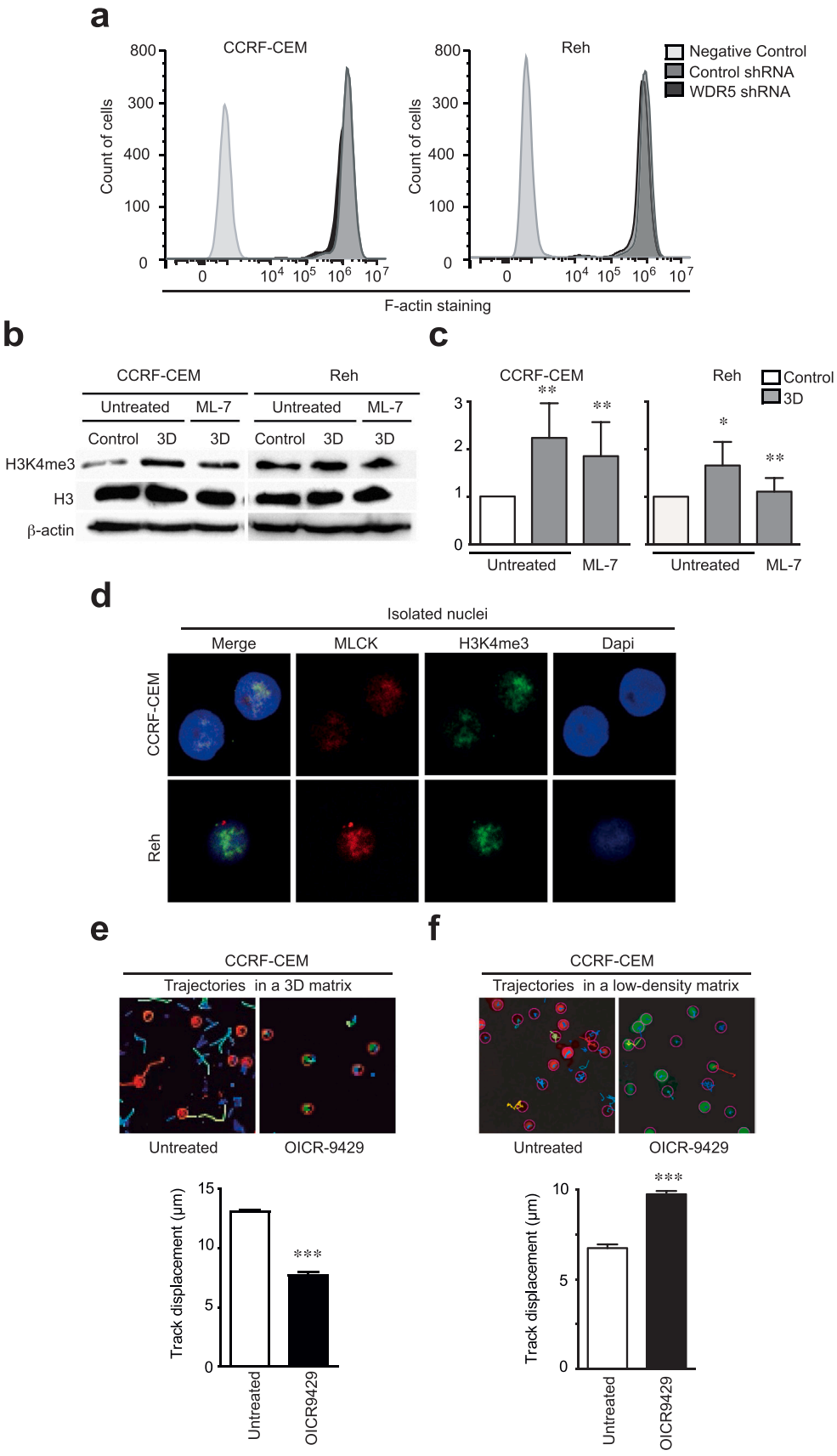

Fig. 4. H3K4 methylation induced by 3D conditions depends on MLCK activity and controls ALL cell displacement in confined conditions. (A) CCRF-CEM and Reh cells transfected with control or WDR5 shRNAs were fixed, and actin polymerization was determined by flow cytometry. (B) CCRF-CEM and Reh cells were treated with 1 μM ml-7 (MLCK inhibitor) for 30 min prior to their culture in 3D conditions. After 1 h, cells were collected and H3K4me3 levels were tested by western blotting. (C) Graph shows the H3K4 methylation levels normalized to loading controls. Mean $n = 3 \pm$ SEM. (D) Isolated nuclei from CCRF-CEM, Reh, and primary ALL cells were seeded on polylysine-coated coverslips. Samples were fixed, permeabilized and the middle section of the nucleus was analyzed by confocal microscopy using specific antibodies. (E) CCRF-CEM cells were pretreated or not with 1 μM OICR-9429, embedded in a high-density 3D collagen gel and allowed to migrate randomly for 3 h. Cell trajectories were tracked and indicated. Graph shows the mean of the track displacement from CCRF-CEM cells migrating in 3D conditions. Mean $n = 3$ replicates $\pm$ SEM. (F) CCRF-CEM cells were pretreated or not with 1 μM OICR-9429, embedded in a low-density collagen gel (0.5 mg/ml) and allowed to migrate as in E. Cell trajectories were tracked and graph shows the mean of the track displacement. Mean $n = 3$ replicates $\pm$ SEM. (***) $P < 0.001$.

targeting WDR5 might affect the levels of MLCK. No change in levels of MLCK was observed in ALL cells treated with OICR-9429 (data not shown) or depleted for WDR5 (Fig. S6D), suggesting that targeting WDR5 might not reduce the myosin activation *per se*. Then, we asked whether MLCK might be present in the nucleus of ALL cells, and described that MLCK localized in those chromatin regions enriched for H3K4 methylation in isolated nuclei from CCRF-CEM and Reh cells (Fig. 4D). To further assess this, we confirmed remarkable levels of this protein in the nuclear fractions of ALL cell lines and primary ALL cells (Fig. S6E).

Cell motility in 3D conditions requires high nuclear deformability in moving cells and might be different than in 2D (Ringer et al., 2017). Given that targeting WDR5 reduced ALL cell dissemination independent of VLA4 and CXCL12 stimulation, we interrogated how leukemia cells move in 3D conditions and whether targeting WDR5 might affect not only the invasiveness but also the effective movement of ALL cells in this environmental condition. We quantified the spontaneous displacements of CCRF-CEM cells embedded in a 3D collagen matrix by live-cell imaging (Movies S1,S2). Our quantitative analysis showed the trajectories of cell migration in 3D environments and indicated that blocking WDR5 reduced the speed and the displacement of CCRF-CEM cells moving in 3D confined conditions (Fig. 4E). Similarly, Reh cells treated with OICR-9429 presented a reduction in their migration through a 3D collagen matrix (Movies S3,S4 and Fig. S7A). To further verify the role of the nucleus in the movement of ALL cells through 3D environments, we performed a similar analysis of ALL cells in 3D low-density collagen gels. A low-density collagen matrix does not require active nuclear deformability from migrating cells and we hypothesized that blocking WDR5 might not reduce their movement in vitro. As expected, the impact of WDR5 inhibition on ALL cell migration across low-density collagen gels was much lower than for restrictive 3D conditions (Movies S5-S8 and Fig. 4F and S7B). Together, our data suggest that OICR-9429 treatment altered the ability of ALL cells to move through confined 3D conditions. Collectively, our data support that targeting WDR5 diminished the capacity of ALL cells to move across 3D environments, which upregulated H3K4 methylation of ALL cells in an MLCK-dependent manner.

Supplementary material related to this article can be found online at doi:10.1016/j.ejcb.2023.151343.

3.5. *H3K4 methylation induced by 3D conditions alters the global chromatin conformation and the nuclear mechanics of leukemia cells*

Firstly, we sought to gain insights into how H3K4 methylation induced by 3D environmental conditions might regulate the global chromatin conformation in ALL cells. We analyzed the chromatin accessibility of CCRF-CEM and Reh cells in suspension or in 3D conditions and found that cells from 3D conditions showed an increased chromatin accessibility to micrococcal DNAse (MNAse) digestion than cells in suspension (Fig. 5A and Fig. S8A). We observed bigger open peaks of nucleosome releasing in those cells cultured in 3D conditions, suggesting that 3D conditions promoted global changes in the chromatin conformation of ALL cells (Fig. 5B). To complement our data and confirm morphological and chromatin changes in the nucleus of ALL cells embedded in 3D conditions, we used electron microscopy to visualize the nuclear morphology of CCRF-CEM cells cultured in suspension and in 3D conditions. As expected from a more open chromatin conformation in 3D culture conditions, we observed that the nucleus of those cells cultured in 3D conditions presented less compacted chromatin regions and more rounded shape than their counterparts from control cells (Fig. 5C).

To determine the changes in the levels and pattern of H3K4 methylation, we performed H3K4me3 ChIP-seq (chromatin immunoprecipitation sequencing) analysis in CCRF-CEM cells cultured in suspension and in 3D conditions and found that the predominant categories enriched in H3K4me3 peaks corresponded to those genes related with cell differentiation, intracellular signaling, oxidative stress and metabolism (Fig. 5D). Since H3K4 methylation might not be required for active gene transcription (Clouaire et al., 2014), we tested whether 3D conditions may promote transcriptional changes related to leukemia progression. To address this, we performed expression profiling on a set of RNAs from CCRF-CEM cells cultured in suspension or in 3D conditions. We identified the differential expression of 165 up- and 84 down-regulated genes in CCRF-CEM cells in 3D conditions with a cut-off of $|\text{Fold Change}| > 1.5$ and a P-value of 0.05 from 21,448 genes (Fig. S8B, Table S2). Our Gene Ontology (GO) enrichment analysis showed changes in transcripts related to transcriptional regulation, cell division and mitosis, and DNA repair (Fig. S8C). To determine the possible association between the global change of H3K4 methylation induced by 3D culture conditions and its potential transcriptional role, we compared the features of the microarray and the ChIPseq analyses (Fig. S8D). Interestingly, we did not find a correlation between H3K4me3 occupancy and transcriptional changes (Fig. 5E), suggesting that the H3K4me3 upregulation induced by 3D conditions might regulate additional non-transcriptional functions in ALL cells. To further validate these observations, we cultured CCRF-CEM cells in 3D conditions and observed that targeting WDR5 altered only 9 transcripts (4 up- and 5 down-regulated) compared to untreated conditions in 3D (Fig. S8E, Table S3). Together, this set of findings indicate that blocking H3K4 methylation had minor effect on the transcriptional changes induced by 3D conditions, supporting the idea that this epigenetic change might control other non-transcriptional functions of ALL cells.

Several non-genomic functions for epigenetic markers have been reported, including the contribution of chromatin structure to nuclear deformability (Bustin and Misteli, 2016). This led us to consider that 3D conditions might regulate the mechanical response of the nucleus. To investigate this, we isolated nuclei from primary ALL cells cultured in suspension or in 3D conditions and determined the mechanical response of the nucleus upon external forces (Fig. 5F). We quantified the nuclear area pre- and post-confinement and found that isolated nuclei from primary ALL cells cultured in 3D conditions showed higher nuclear deformability upon external compression than isolated nuclei from control conditions (Fig. 5G). To determine the fundamental impact of H3K4 methylation on the mechanical changes induced by 3D conditions, we cultured control and OICR-9429-treated ALL cells in suspension or in 3D conditions. Our results confirmed that 3D conditions increased the nuclear deformability of ALL cells, and targeting WDR5 reduced this mechanical effect (Fig. 5H). Similarly, OICR-9429 treatment also reduced the impact of 3D culture conditions on the nuclear deformability of primary ALL cells (Fig. S9A). Consistent with these findings, we demonstrated that WDR5 depletion also abrogated the nuclear deformability induced by 3D conditions in ALL cells (Fig. S9B). Together, these data support that 3D conditions altered the global chromatin structure, the morphology, and the mechanical properties of the nucleus of ALL cells.

4. Discussion

Cell migration through 3D environments is a critical step in multiple physiological and pathological processes such as development, inflammation, wound healing, and cancer invasion (Kirby and Lammerding, 2018). To penetrate into protective niches, such as the bone marrow or the central nervous system, cancer cells must respond to biochemical and mechanical signals induced by their surrounding 3D environment (Chiarini et al., 2016). Therefore, identifying novel molecules that regulate molecular and mechanical pathways for tumor dissemination is an important direction to developing more effective therapeutic options. In this study, we have defined a mechanism used by ALL cells to control cell invasiveness through 3D environments by promoting H3K4 methylation and altering the chromatin structure and the mechanical properties of the nucleus.

3D culture conditions lead to transcriptional and epigenetic changes, by altering the ratio between hetero and euchromatin (Stephens et al.,

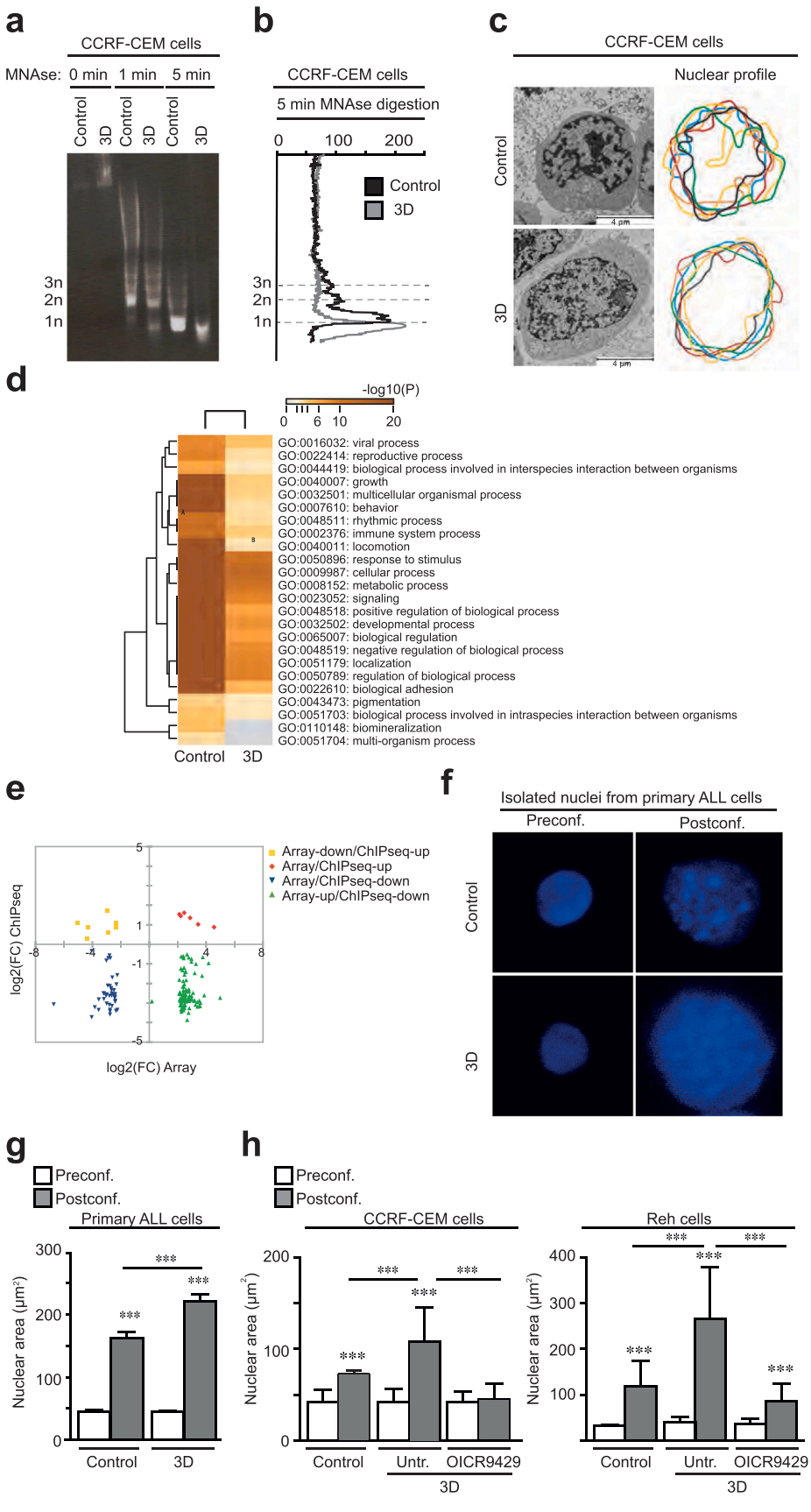

Fig. 5. 3D conditions alter the global chromatin conformation and the nuclear mechanics in ALL cells. (A) CCRF-CEM cells were cultured in suspension or in 3D conditions before digesting their DNA with micrococcal nuclease at different times. Mono (1 n), di (2 n), and tri (3 n) nucleosomes are indicated. (B) Graph shows the nucleosomal releasing profile of CCRF-CEM cells in suspension or in 3D conditions at 5 min after micrococcal digestion. (C) CCRF-CEM cells cultured in suspension or in 3D conditions were collected and processed for thin-section electron microscopy to visualize the nuclear morphology. Plot show changes in the nuclear morphology of CCRF-CEM cells cultured in suspension or in 3D conditions ($n = 6$ representative cells). (D) Graph shows the top gene ontology (GO) enrichment results from H3K4me3 ChIPseq analysis of CCRF-CEM cultured in suspension or in 3D conditions. (E) Correlation plot of differentially expressed transcripts from the microarray experiment and the H3K4me3 occupancy from ChIPseq assays in CCRF-CEM cultured in 3D conditions. (F) Isolated nuclei from primary ALL cells cultured in suspension or in 3D conditions were stained and seeded on polylysine-coated coverslips. Confocal sections of the nuclei were taken before (Preconf.) and after (Postconf.) external compression of the nucleus. (G) Graph shows the mean average of the nuclear area in (F). Mean $n = 22–46$ isolated nuclei $\pm$ SEM. (H) CCRF-CEM and Reh cells were treated with 1 μM OICR-9294 and culture in 3D conditions. Then, their nuclei were isolated, stained and the nuclear deformability was determined by external pressure. Mean $n = 53–71$ isolated nuclei $\pm$ SEM. (***) $P < 0.001$.

2019; Segal et al., 2018). In agreement with this, we have determined that 3D confined conditions induced upregulation of H3K4me3 of ALL cells. This epigenetic change is critical for multiple functions of normal lymphocytes and hematological malignancies, including cell migration, DNA methylation, stem cell fate, and resistance to DNA damage stress (Ge et al., 2016; Wong et al., 2015; Scalea et al., 2020). Our observations indicate that the H3K4 methylation induced by 3D conditions in ALL cells was reversible, as leukemia cells recovered the basal levels in the absence of any 3D environment. It means that H3K4 methylation might have a protective and promigratory role when leukemia cells are moving through confined conditions, which might be particularly important in leukemia invasiveness as confined migration control genomic instability and cell cycle progression (Denais et al., 2016; Uroz et al., 2018). Targeting WDR5 with the specific inhibitor OICR-9429 blocks cancer cell proliferation and growth (Zhu et al., 2015). It has been reported that WDR5 regulates the invasive properties of breast cancer cells without inhibiting cell adhesion (Kim et al., 2014). In accordance with this finding, we observed that targeting WDR5 severely reduced cell migration across 3D environments. By using an *in vivo* model to study ALL spreading through different tissues, we confirmed that targeting WDR5 reduced ALL cell invasiveness and homing into the spleen and the bone marrow.

ALL infiltration into the interstitial space and different organs is a multistep function that requires many external stimuli including chemokines and integrins, which have been reported as critical for the migration and invasiveness of ALL cells (Redondo-Muñoz et al., 2019). As epigenetic changes have been defined as new biomarkers and potential therapeutic targets in ALL (Mar et al., 2014), we explored a potential correlation between WDR5 and CXCR4 or VLA4, two cell receptors critical for ALL cell invasiveness a positive (Shalapour et al., 2011). We found a positive correlation of mRNA levels between WDR5 and CXCR4 in clinical samples; however, our data suggested that the inhibitory effect of WDR5 inhibition on ALL cells was not mediated by affecting actin polymerization, nor the expression of the integrin VLA4, S1PR1, CCR7 or CXCR4 in ALL cells. This suggests that the expression of these molecules and WDR5 might serve to promote leukemia cell invasion at different stages or for specific subtypes of ALL. Interestingly, when we analyzed the chemotaxis of ALL cells to CXCL12 and FBS, we observed an increment in the migratory capacity of these cells. Besides its role in 3D cell migration, WDR5 modulates other potential cytoplasmic targets and multiple signaling pathways (Huang et al., 2020; Ge et al., 2016; Chi et al., 2022; Kulkarni et al., 2018), which might participate in the effect of WDR5 inhibition on the chemotactic response of ALL cells. Furthermore, it has been reported that VLA4 and CXCL12 signals promote other epigenetic changes, such as H3K9 methylation, in ALL cells and leukocytes (Madrazo et al., 2018 and 2022; Calì et al., 2022); therefore, we cannot exclude other molecular mechanisms driving the dual effect observed for WDR5 targeting in 3D or chemotactic migration and future experiments might be relevant to clarify this point.

Mechanistically, the actin dynamics and myosin contractility translate intracellular signals and forces critical for hematopoiesis (Shin et al., 2014), leukemia infiltration (Wigton et al., 2016), and for nuclear changes during cell migration through complex environments (Jain et al., 2013). Our results revealed that 3D conditions promoted myosin phosphorylation and an upregulation of H3K4me3 of ALL cells through MLCK activity. It has been reported the functional link between actomyosin contractility and H3K4 methylation (Downing et al., 2013); herein, we demonstrated that MLCK localized in the vicinity of H3K4me3 regions in the nucleus of leukemia cells. This also agrees with previous observations of MLCK and myosin in the nucleus of several cell types (Leitman et al., 2011), which suggests a potential role of this kinase in chromatin homeostasis and conformation.

WDR5 interacts with the protooncogene myc and other transcription factors to drive tumorigenesis and cancer progression (Sun et al., 2015; Thomas et al., 2015); nonetheless, we did not find significant changes in the expression of c-Myc at the studied times. Our transcriptional analysis of ALL cells embedded in 3D conditions showed potential alterations in genes related to DNA repair and cell cycle. These transcriptional changes might be connected to microenvironmental signals that promote clonal genetic differences, chromatin instability, and cell resistance to drug therapy at specific niches (Swaminathan et al., 2015). Moreover, WDR5 binds to other proteins, including nuclear factors and cytoplasmic proteins regulating cell transcription, division, and morphology (Chi et al., 2022; Kulkarni et al., 2018; Bailey et al., 2015). It is possible that these complexes might participate in additional functions or in other biological aspects of ALL cells rather than 3D migration. In fact, we did not see differences in the cell cycle of ALL cells induced by WDR5 targeting; but we cannot discard that cyclin D1 might increase at longer times or even favors changes in cell cycle. To rule out how H3K4me3 induced by 3D conditions might be affecting directly the transcriptional program of ALL cells, we analyze the correlation between H3K4me3 ChIPseq and the transcriptional analyses. Interestingly, we did not find a significant direct correlation, which aligns with other studies where histone methylation might alter the mechanical response of the nucleus independently of any transcriptional regulation (Madrazo et al., 2022; Nava et al., 2020). This might indicate other additional functions for H3K4 methylation rather than just transcriptional activation; although we cannot discard that other molecules might contribute to multiple functions of ALL cells in 3D at longer times, and or under other specific cellular confinement. In agreement with this idea, it has been reported that the loss of H3K4me3 has minor effects on transcription, and might regulate other functional effects such as DNA replication stress (Margaritis et al., 2012). It is well described that the mechanical properties of the nucleus are defined by the nuclear lamina and the chromatin structure (Stephens et al., 2018). Lamin expression in lymphocytes is highly restrictive (Saez et al., 2020), and the chromatin compaction has been reported as fundamental in the mechanical response of normal and tumor cells (Segal et al., 2018; Zhang et al., 2016). Our results demonstrated that cells embedded in 3D conditions altered the nuclear morphology, and the global chromatin structure and showed different nuclear deformability upon external compression, which was dependent on WDR5 activity. The nuclear deformability controls cancer cell migration in confined conditions, such as 3D environments (Athirasala et al., 2017) and, in agreement with these observations, we have demonstrated that targeting WDR5 diminished the migration of leukemia cells through confined conditions that require active nuclear deformability. In contrast, when leukemia cells were embedded in a low-density collagen matrix that might not require nuclear deformation, WDR5 inhibition had a minor inhibitory effect on ALL cell migration or even increased for the displacement of CCRF-CEM cells. This aligns with our observation of the effect of WDR5 inhibition on the chemotactic response of ALL cells and suggests that other potential mechanisms might be controlled by WDR5 during the migration of ALL cells across different microenvironments. Together, our data indicate the particular effect of WDR5 targeting during leukemia cell migration in 3D and anticipate other potential effects to explore depending on the microenvironment of migrating cancer cells.

5. Conclusions

In summary, our study emphasized on the nuclear mechanism used by leukemia cells to sense and move through 3D spaces. This mechanism evolves rapid dynamic adaptation of H3K4 methylation, alteration of the morphology, and the mechanical properties of the nucleus of moving cells. Our findings highlight a relevant function of H3K4 methylation for ALL cell infiltration and plasticity that might provide therapeutic possibilities against leukemia dissemination.

Ethics approval and consent to participate

This study was reviewed and approved by the ethics committee of the

CSIC and Hospital Niño Jesús, and written informed consent was obtained from all parents, according to the Helsinki Declaration of 1975. All procedures for animal experiments were approved by the Committee on the Use and Care of Animals and carried out in strict accordance with the institution guidelines and the European and Spanish legislations for laboratory animal care.

Funding

This research was supported by a FPI Scholarship 2018 (Ministerio de Ciencia e Innovacion/MICINN, Agencia Estatal de Investigacion/AEI y Fondo Europeo de Desarrollo Regional/FEDER) to R.G.N.; JAE Intro 2022 (Agencia Estatal Consejo Superior de Investigaciones Científicas, Conexión CSIC Cancer, JAEINT22_EX_0263) to M.P.C.R; grants from Asociación Pablo Ugarte to M.R.; and grants from 2020 Leonardo Grant for Researchers and Cultural Creators (BBVA Foundation), Ayuda de contratación de ayudante de investigación PEJ-2020-AI/BMD-19152 (Comunidad de Madrid), and the Ministerio de Ciencia e Innovacion (MICINN) Agencia Estatal de Investigacion (AEI) y Fondo Europeo de Desarrollo Regional (FEDER) (SAF2017–86327-R and PDI2020–118525RB-I00) to J.R.M.

CRediT authorship contribution statement

R. González-Novo: Conceptualization, Investigation, Formal analysis, Writing - Review & Editing **A. de Lope-Planelles:** Investigation **M. P. Cruz Rodríguez:** Investigation **A. González-Murillo,** Methodology, Investigation, Resources**, E. Madrazo:** Investigation **D. Acitores:** Investigation **M. García de Lacoba:** Formal analysis, Data Curation. **M. Ramírez:** Conceptualization, Writing - Review & Editing, Funding acquisition **J. Redondo-Muñoz:** Conceptualization, Supervision, Writing-Original draft preparation, Funding acquisition.

Declaration of Competing Interest

The authors declare that they have no known competing financial interests or personal relationships that could have appeared to influence the work reported in this paper.

Data availability

Data will be made available on request.

Acknowledgments

ALL primary cells were obtained from patients under 16 years old with informed consent for research purposes and approved by the Ethics Committee for Medical Research (IRB) at Hospital Universitario Niño Jesús and CSIC. All experiments involving animals were approved by the OEBA (Organ for Evaluating Animal Wellbeing) at CIB Margarita Salas and Madrid Regional Department of Environment, with reference PROEX 228.4/21. The authors thank the Microscopy Unit of Instituto de Investigación Biosanitaria Gregorio Marañón (IiSGM) for assistance with confocal and videomicroscopy analyses. The authors are also grateful to the EM and Animal Facilities of platforms of the CIB Margarita Salas for their assistance and support with the EM and *in vivo* experiments. The UCM-Genomic CAI Unit for their assistance with microarray experiments.

Author Contribution Statement

R.G.N., A.dL.P., M.P.C.R., A.G.M., D.A., E.M., conducted experiments. M.G.dL. performed ChIPSeq analysis. M.R., provided primary ALL samples, clinical characterization and contributed to clinical data interpretation. J.R.M designed and supervised the experiments, wrote the paper, and provided financing.

Consent for publication

All the authors have read and approved the fnal manuscript.

Appendix A. Supporting information

Supplementary data associated with this article can be found in the online version at doi:10.1016/j.ejcb.2023.151343.

References

Almamun, M., Levinson, B.T., van Swaay, A.C., Johnson, N.T., McKay, S.D., Arthur, G.L., et al., 2015. Integrated methylome and transcriptome analysis reveals novel regulatory elements in pediatric acute lymphoblastic leukemia. Epigenetics 10, 882–890.

Athirasala, A., Hirsch, N., Buxboim, A., 2017. Nuclear mechanotransduction: sensing the force from within. Curr. Opin. Cell Biol. 46, 119–127.

Bailey, J.K., Fields, A.T., Cheng, K., Lee, A., Wagenaar, E., Lagrois, R., Schmidt, B., Xia, B., Ma, D., 2015. WD repeat-containing protein 5 (WDR5) localizes to the midbody and regulates abscission. J. Biol. Chem. 290, 8987–9001.

Buonamici, S., Trimarchi, T., Ruocco, M.G., Reavie, L., Cathelin, S., Mar, B.G., Klinakis, A., Lukyanov, Y., Tseng, J.C., Sen, F., et al., 2009. CCR7 signalling as an essential regulator of CNS infiltration in T-cell leukaemia. Nature 459, 1000–1004.

Bustin, M., Misteli, T., 2016. Nongenetic functions of the genome. Science 352, 6933.

Calì, B., Deygas, M., Munari, F., Marcuzzi, E., Cassará, A., Toffali, L., Vetralla, M., Bernard, M., Piel, M., Gagliano, O., Mastrogiovanni, M., Laudanna, C., Elvassore, N., Molon, B., Vargas, P., Viola, A., 2022. Atypical CXCL12 signaling enhances neutrophil migration by modulating nuclear deformability. Sci. Signal 15, eabk2552.

Chi, Z., Zhang, B., Sun, R., Wang, Y., Zhang, L., Xu, G., 2022. USP44 accelerates the growth of T-cell acute lymphoblastic leukemia through interacting with WDR5 and repressing its ubiquitination. Int. J. Med. Sci. 19, 2022–2032.

Chiarini, F., Lonetti, A., Evangelisti, C., Buontempo, F., Orsini, E., Evangelisti, C., et al., 2016. Advances in understanding the acute lymphoblastic leukemia bone marrow microenvironment: from biology to therapeutic targeting. Biochim. Biophys. Acta 1863, 449–463.

Chong, S.Y., Cutler, S., Lin, J.J., Tsai, C.H., Tsai, H.K., Biggins, S., et al., 2020. H3K4 methylation at active genes mitigates transcription-replication conflicts during replication stress. Nat. Commun. 11, 809.

Clouaire, T., Webb, S., Skene, P., Illingworth, R., Kerr, A., Andrews, R., et al., 2012. Cfp1 integrates both CpG content and gene activity for accurate H3K4me3 deposition in embryonic stem cells. Genes Dev. 26, 1714–1728.

Clouaire, T., Webb, S., Bird, A., 2014. Cfp1 is required for gene expression-dependent H3K4 trimethylation and H3K9 acetylation in embryonic stem cells. Genome Biol. 15, 451.

Corcione, A., Arduino, N., Ferretti, E., Pistorio, A., Spinelli, M., Ottonello, L., Dallegri, F., Basso, G., Pistoia, V., 2006. Chemokine receptor expression and function in childhood acute lymphoblastic leukemia of B-lineage. Leuk. Res. 30, 365–372.

Crazzolara, R., Kreczy, A., Mann, G., Heitger, A., Eibl, G., Fink, F.M., et al., 2001. High expression of the chemokine receptor CXCR4 predicts extramedullary organ infiltration in childhood acute lymphoblastic leukemia. Br. J. Haematol. 115, 545–553.

Dahl, K.N., Ribeiro, A.J., Lammerding, J., 2008. Nuclear shape, mechanics, and mechanotransduction. Circ. Res. 102, 1307–1318.

Denais, C.M., Gilbert, R.M., Isermann, P., McGregor, A.L., te Lindert, M., Weigelin, B., et al., 2016. Nuclear envelope rupture and repair during cancer cell migration. Science 352, 353–358.

Dou, Y., Milne, T.A., Ruthenburg, A.J., Lee, S., Lee, J.W., Verdine, G.L., et al., 2006. Regulation of MLL1 H3K4 methyltransferase activity by its core components. Nat. Struct. Mol. Biol. 13, 713–719.

Downing, T.L., Soto, J., Morez, C., Houssin, T., Fritz, A., Yuan, F., et al., 2013. Biophysical regulation of epigenetic state and cell reprogramming. Nat. Mater. 12, 1154–1162.

Figueroa, M.E., Chen, S.C., Andersson, A.K., Phillips, L.A., Li, Y., Sotzen, J., et al., 2013. Integrated genetic and epigenetic analysis of childhood acute lymphoblastic leukemia. J. Clin. Investig. 123, 3099–3111.

García-Bernal, D., Redondo-Muñoz, J., Dios-Esponera, A., Chèvre, R., Bailón, E., Garayoa, M., Arellano-Sánchez, N., Gutierrez, N.C., Hidalgo, A., García-Pardo, A., Teixidó, J., 2013. Sphingosine-1-phosphate activates chemokine-promoted myeloma cell adhesion and migration involving α4β1 integrin function. J. Pathol. 229, 36–48.

Ge, Z., Song, E.J., Kawasawa, Y.I., Li, J., Dovat, S., Song, C., 2016. WDR5 high expression and its effect on tumorigenesis in leukemia. Oncotarget 7, 37740–37754.

Golan, K., Kollet, O., Lapidot, T., 2013. Dynamic cross talk between S1P and CXCL12 regulates hematopoietic stem cells migration, development and bone remodeling. Pharmaceuticals 6, 1145–1169.

Grebien, F., Vedadi, M., Getlik, M., Giambruno, R., Grover, A., Avellino, R., et al., 2015. Pharmacological targeting of the Wdr5-MLL interaction in C/EBPα N-terminal leukemia. Nat. Chem. Biol. 11, 571–578.

Hu, D., Gao, X., Cao, K., Morgan, M.A., Mas, G., Smith, E.R., et al., 2017. Not All H3K4 methylations are created equal: Mll2/COMPASS dependency in primordial germ cell specification. Mol. Cell. 65, 460–475 e6.

Huang, D., Chen, X., Chen, X., Qu, Y., Wang, Y., Yang, Y., et al., 2020. WDR5 promotes proliferation and correlates with poor prognosis in oesophageal squamous cell carcinoma. Onco Targets Ther. 13, 10525–10534.

Inaba, H., Greaves, M., Mullighan, C.G., 2013. Acute lymphoblastic leukemia. Lancet 381, 1943–1955.
Jain, N., Iyer, K.V., Kumar, A., Shivashankar, G.V., 2013. Cell geometric constraints induce modular gene-expression patterns via redistribution of HDAC3 regulated by actomyosin contractility. Proc. Natl. Acad. Sci. USA 110, 11349–11354.
Kelley, L.C., Chi, Q., Cáceres, R., Hastie, E., Schindler, A.J., Jiang, Y., et al., 2019. Adaptive F-actin polymerization and localized ATP production drive basement membrane invasion in the absence of MMPs. Dev. Cell. 48, 313–328.
Kim, J.Y., Banerjee, T., Vinckevicius, A., Luo, Q., Parker, J.B., Baker, M.R., et al., 2014. A role for WDR5 in integrating threonine 11 phosphorylation to lysine 4 methylation on histone H3 during androgen signaling and in prostate cancer. Mol. Cell 54, 613–625.
Kirby, T.J., Lammerding, J., 2018. Emerging views of the nucleus as a cellular mechanosensor. Nat. Cell Biol. 20, 373–381.
Kouzarides, T., 2007. Chromatin modifications and their function. Cell 128, 693–705.
Kulkarni, S.S., Griffin, J.N., Date, P.P., Liem Jr., K.F., Khokha, M.K., 2018. WDR5 stabilizes actin architecture to promote multiciliated cell formation. Dev. Cell 46, 595–610.
Leitman, E.M., Tewari, A., Horn, M., Urbanski, M., Damanakis, E., Einheber, S., et al., 2011. MLCK regulates Schwann cell cytoskeletal organization, differentiation and myelination. J. Cell Sci. 124, 3784–3796.
Madrazo, E., Ruano, D., Abad, L., Alonso-Gómez, E., Sánchez-Valdepeñas, C., González-Murillo, A., et al., 2018. G9a correlates with VLA-4 integrin and influences the migration of childhood acute lymphoblastic leukemia cells. Cancers 10, 325.
Madrazo, E., González-Novo, R., Ortiz-Placín, C., García de Lacoba, M., González-Murillo, A., Ramírez, M., et al., 2022. Fast H3K9 methylation promoted by CXCL12 contributes to nuclear changes and invasiveness of T-acute lymphoblastic leukemia cells. Oncogene 41, 1324–1336.
Mar, B.G., Bullinger, L.B., McLean, K.M., Grauman, P.V., Harris, M.H., Stevenson, K., et al., 2014. Mutations in epigenetic regulators including SETD2 are gained during relapse in pediatric acute lymphoblastic leukemia. Nat. Commun. 5, 3469.
Margaritis, T., Oreal, V., Brabers, N., Maestroni, L., Vitaliano-Prunier, A., Benschop, J.J., et al., 2012. Two distinct repressive mechanisms for histone 3 lysine 4 methylation through promoting 3'-end antisense transcription. PLOS Genet. 8, e1002952.
Nava, M.M., Miroshnikova, Y.A., Biggs, L.C., Whitefield, D.B., Metge, F., Boucas, J., et al., 2020. Heterochromatin-driven nuclear softening protects the genome against mechanical stress-induced damage. Cell 181, 800–817.
Portela, A., Esteller, M., 2010. Epigenetic modifications and human disease. Nat. Biotech. 28, 1057–1068.
Punzi, S., Balestrieri, C., D'Alesio, C., Bossi, D., Dellino, G.I., Gatti, E., et al., 2019. WDR5 inhibition halts metastasis dissemination by repressing the mesenchymal phenotype of breast cancer cells. Breast Cancer Res. 21, 123.
Redondo-Muñoz, J., García-Pardo, A., Teixidó, J., 2019. Molecular players in hematologic tumor cell trafficking. Front. Immunol. 10, 156.
Ringer, P., Colo, G., Fassler, R., Grashoff, C., 2017. Sensing the mechano-chemical properties of the extracellular matrix. Matrix Biol. 64, 6–16.
Saez, A., Herrero-Fernandez, B., Gomez-Bris, R., Somovilla-Crespo, B., Rius, C., Gonzalez-Granado, J.M., 2020. Lamin A/C and the immune system: one intermediate filament, many faces. Int. J. Mol. Sci. 21, 6109.
Scalea, S., Maresca, C., Catalanotto, C., Marino, R., Cogoni, C., Reale, A., et al., 2020. Modifications of H3K4 methylation levels are associated with DNA hypermethylation in acute myeloid leukemia. FEBS J. 287, 1155–1175.
Segal, T., Salmon-Divon, M., Gerlitz, G., 2018. The heterochromatin landscape in migrating cells and the importance of H3K27me3 for associated transcriptome alterations. Cells 7, 205.
Shalapour, S., Hof, J., Kirschner-Schwabe, R., Bastian, L., Eckert, C., Prada, J., et al., 2011. High VLA-4 expression is associated with adverse outcome and distinct gene expression changes in childhood B-cell precursor acute lymphoblastic leukemia at first relapse. Haematologica 96, 1627–1635.
Shin, J.W., Buxboim, A., Spinler, K.R., Swift, J., Christian, D.A., Hunter, C.A., et al., 2014. Contractile forces sustain and polarize hematopoiesis from stem and progenitor cells. Cell Stem Cell 14, 81–93.
Shivashankar, G.V., 2011. Mechanosignaling to the cell nucleus and gene regulation. Annu. Rev. Biophys. 40, 361–378.
Spiegel, S., Kolesnick, R., 2002. Sphingosine 1-phosphate as a therapeutic agent. Leukemia 16, 1596–1602.
Stephens, A.D., Liu, P.Z., Banigan, E.J., Almassalha, L.M., Backman, V., Adam, S.A., et al., 2018. Chromatin histone modifications and rigidity affect nuclear morphology independent of lamins. Mol. Biol. Cell. 29, 220–233.
Stephens, A.D., Liu, P.Z., Kandula, V., Chen, H., Almassalha, L.M., Herman, C., et al., 2019. Physicochemical mechanotransduction alters nuclear shape and mechanics via heterochromatin formation. Mol. Biol. Cell. 30, 2320–2330.
Sun, Y., Bell, J.L., Carter, D., Gherardi, S., Poulos, R.C., Milazzo, G., Wong, J.W.H., et al., 2015. WDR5 supports an N-Myc transcriptional complex that drives a protumorigenic gene expression signature in neuroblastoma. Cancer Res. 75, 5143–5154.
Swaminathan, S., Klemm, L., Park, E., Papaemmanuil, E., Ford, A., Kweon, S.M., et al., 2015. Mechanisms of clonal evolution in childhood acute lymphoblastic leukemia. Nat. Immunol. 16, 766–774.
Tan, X., Chen, S., Wu, J., Lin, J., Pan, C., Ying, X., et al., 2017. PI3K/AKT-mediated upregulation of WDR5 promotes colorectal cancer metastasis by directly targeting ZNF407. Cell Death Dis. 8, e2686.
Thomas, L.R., Wang, Q., Grieb, B.C., Phan, J., Foshage, A.M., Sun, Q., et al., 2015. Interaction with WDR5 promotes target gene recognition and tumorigenesis by MYC. Mol. Cell 58, 440–521.
Trievel, R.C., Shilatifard, A., 2009. WDR5, a complexed protein. Nat. Struct. Mol. Biol. 16, 678–680.
Uroz, M., Wistorf, S., Serra-Picamal, X., Conte, V., Sales-Pardo, M., Roca-Cusachs, P., et al., 2018. Regulation of cell cycle progression by cell-cell and cell-matrix forces. Nat. Cell Biol. 20, 646–654.
Vadillo, E., Dorantes-Acosta, E., Pelayo, R., Schnoor, M., 2018. T cell acute lymphoblastic leukemia (T-ALL): New insights into the cellular origins and infiltration mechanisms common and unique among hematologic malignancies. Blood Rev. 32, 36–51.
Wang, P., Dreger, M., Madrazo, E., Williams, C.J., et al., 2018. WDR5 modulates cell motility and morphology and controls nuclear changes induced by a 3D environment. Proc. Natl. Acad. Sci. USA 115, 8581–8586.
Wigton, E.J., Thompson, S.B., Long, R.A., Jacobelli, J., 2016. Myosin-IIA regulates leukemia engraftment and brain infiltration in a mouse model of acute lymphoblastic leukemia. J. Leukoc. Biol. 100, 143–153.
Wolf, K., Te Lindert, M., Krause, M., Alexander, S., Te Riet, J., Willis, A.L., et al., 2013. Physical limits of cell migration: control by ECM space and nuclear deformation and tuning by proteolysis and traction force. J. Cell Biol. 201, 1069–1084.
Wong, S.H., Goode, D.L., Iwasaki, M., Wei, M.C., Kuo, H.P., Zhu, L., et al., 2015. The H3K4-methyl epigenome regulates leukemia stem cell oncogenic potential. Cancer Cell 28, 198–209.
Yamada, K.M., Sixt, M., 2019. Mechanisms of 3D cell migration. Nat. Rev. Mol. Cell Biol. 20, 738–752.
Zhang, X., Cook, P.C., Zindy, E., Williams, C.J., Jowitt, T.A., Streuli, C.H., et al., 2016. Integrin α4β1 controls G9a activity that regulates epigenetic changes and nuclear properties required for lymphocyte migration. Nucleic Acids Res. 44, 3031–3044.
Zhu, J., Sammons, M.A., Donahue, G., Dou, Z., Vedadi, M., Getlik, M., et al., 2015. Gain-of-function p53 mutants co-opt chromatin pathways to drive cancer growth. Nature 525, 206–211.